HHS Public Access

Author manuscript

Cell Rep. Author manuscript; available in PMC 2020 October 19.

Published in final edited form as:

Cell Rep. 2020 September 29; 32(13): 108196. doi:10.1016/j.celrep.2020.108196.

Divergent Roles of PI3K Isoforms in PTEN-Deficient Glioblastomas

Shaozhen Xie[1,2,7], **Jing Ni**[1,2,7], **J. Ricardo McFaline-Figueroa**[1,3,4], **Yanzhi Wang**[1], **Roderick T. Bronson**[5], **Keith L. Ligon**[3,4], **Patrick Y. Wen**[3,4], **Thomas M. Roberts**[1,2,*], **Jean J. Zhao**[1,2,6,8,*]

[1]Department of Cancer Biology, Dana-Farber Cancer Institute, Boston, MA 02215, USA

[2]Department of Biological Chemistry and Molecular Pharmacology, Harvard Medical School, Boston, MA 02215, USA

[3]Center for Neuro-Oncology, Dana-Farber Cancer Institute, Boston, MA 02215, USA

[4]Departments of Medical Oncology and Oncologic Pathology, Dana-Farber Cancer Institute, Boston, MA 02215, USA

[5]Dana-Farber/Harvard Cancer Center Rodent Histopathology Core, Boston, MA 02215, USA

[6]Broad Institute of Harvard and MIT, Cambridge, MA 02142, USA

[7]These authors contributed equally

[8]Lead Contact

SUMMARY

Loss of PTEN, the negative regulator of PI3K activity, is frequent in glioblastomas (GBMs). However, the role of the two major PI3K isoforms, p110α and p110β, in PTEN-deficient gliomagenesis remains unknown. We show that PTEN-deficient GBM largely depends on p110α for proliferation and p110β for migration. Genetic ablation of either isoform delays tumor progression in mice, but only ablating both isoforms completely blocks GBM driven by the concurrent ablation of *Pten* and *p53*. BKM120 (buparlisib) treatment only modestly prolongs survival in mice bearing intracranial *Pten/p53* null tumors due to partial pathway inhibition.

*Correspondence: thomas_roberts@dfci.harvard.edu (T.M.R.), jean_zhao@dfci.harvard.edu (J.J.Z.).

AUTHOR CONTRIBUTIONS

S.X., J.N., T.M.R., and J.J.Z. conceived and designed the experiments. S.X., J.N., and Y.W. performed the experiments and collected the data. S.X., J.N., J.R.M.F., R.T.B., K.L.L., P.Y.W., T.M.R., and J.J.Z. analyzed the data. S.X., J.N., J.R.M.F., K.L.L., P.Y.W., T.M.R., and J.J.Z. wrote and reviewed the paper. All of the authors approved the final manuscript.

SUPPLEMENTAL INFORMATION

Supplemental Information can be found online at https://doi.org/10.1016/j.celrep.2020.108196.

DECLARATION OF INTERESTS

J.N. consults for Geode Therapeutics. K.L.L. is a founder and board member of Travera LLC, a consultant for BMS, Integragen, and Rarecyte, and has received research support from BMS, Lilly, Novartis, Amgen, and Deciphera. P.Y.W receives research support from Agios, AstraZeneca/Medimmune, Beigene, Celgene, Eli Lily, Genentech/Roche, Kazia, MediciNova, Merck, Novartis, Oncoceutics, Vascular Biogenics, and VBI Vaccines, is on the advisory boards of Agios, AstraZeneca, Bayer, Blue Earth Diagnostics, Immunomic Therapeutics, Karyopharm, Kiyatec, Puma, Taiho, Vascular Biogenics, Deciphera, VBI Vaccines, Tocagen, Voyager, QED, Elevate Bio, Integral Health, and Imvax, has received speaker fees from Merck and Prime Oncology, and is an editor for Elsevier and UpToDate. T.M.R. consults for and has received research grants from Novartis and is a member of the corporate boards of Crimson Biotech and Geode Therapeutics. J.J.Z. is a founder and board director of Crimson Biotech and Geode Therapeutics. The other authors declare no competing interests.

BKM120 extends the survival of mice bearing intracranial tumors in which p110β, but not p110α, has been genetically ablated in the *Pten/p53* null glioma, indicating that BKM120 fails to inhibit p110β effectively. Our study suggests that the failure of PI3K inhibitors in GBM may be due to insufficient inhibition of p110β and indicates a need to develop brain-penetrant p110α/β inhibitors.

In Brief

Xie et al. show that p110α and p110β isoforms of PI3K play overlapping and divergent roles in PTEN-deficient glioblastomas, suggesting the importance of blocking both PI3K isoforms to effectively treat PTEN-deficient glioblastomas. Moreover, this study also provides a potential mechanism explaining the failure of BKM120 in the clinic.

Graphical Abstract

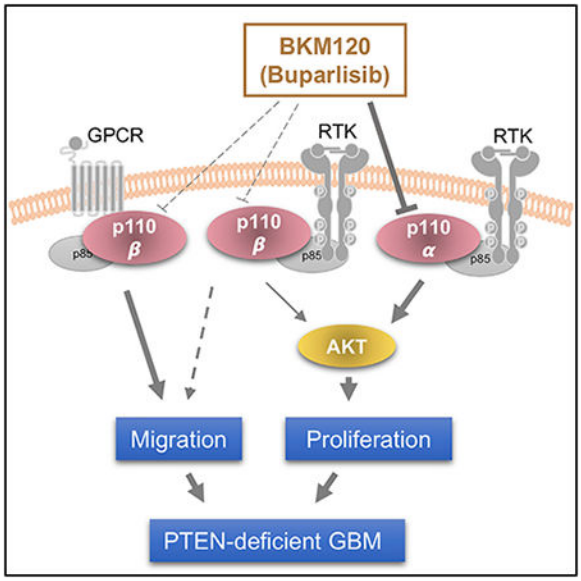

INTRODUCTION

Glioblastoma (GBM) is the most common and malignant primary brain tumor in adults. The current treatment options for GBM only modestly extend survival, despite aggressive multimodality care (Wen et al., 2020). New therapies require a better understanding of GBM biology. The loss of PTEN (phosphatase and tensin homolog) through genetic or epigenetic alterations happens frequently in GBM and is associated with therapeutic resistance (Brennan et al., 2013; Cancer Genome Atlas Research Network, 2008). PTEN is a major tumor suppressor and the key negative regulator of class I phosphatidylinositol 3-kinase (PI3K) activity (Bergholz et al., 2018; Fruman et al., 2017; Thorpe et al., 2015).

The small family of PI3Ks is the only class of enzymes capable of phosphorylating phosphoinositides at the 3’ position of the inositol ring. The family is divided into three classes according to substrate specificity and subunit makeup. Among them, class IA PI3Ks are clearly involved in cancer. Class IA PI3Ks convert phosphatidylinositol 4,5-bisphosphate

(PIP2) to phosphatidylinositol (3,4,5)-trisphosphate (PIP3), an intracellular second messenger that activates multiple effector proteins, including AKT. PTEN is the lipid phosphatase that counteracts the activity of PI3K by dephosphorylating the 3' position of PIP3, thus converting it back into PIP2. The class IA PI3Ks consist of a p110 catalytic subunit and a p85 adaptor subunit. There are three p110 catalytic isoforms, p110α, p110β, and p110δ, encoded by *PIK3CA, PIK3CB*, and *PIK3CD*, respectively. The p110α and p110β isoforms are expressed ubiquitously, whereas p110δ is mainly expressed in leukocytes. Despite their high homologies, the p110 isoforms regulate distinct physiological and pathological functions (Bergholz et al., 2018; Fruman et al., 2017; Thorpe et al., 2015). While p110α is activated by receptor tyrosine kinase (RTK) signaling, p110β mediates both RTK and G protein-coupled receptors (GPCR) signaling. Recent studies have suggested that most solid tumors are partially dependent on one of the p110 isoforms for survival, with the isoform involved varying with tumor type and genetic background. Broadly speaking, most tumors driven by RTK or Ras depend on p110α (Bergholz et al., 2018; Utermark et al., 2014), while tumors driven by PTEN loss depend on p110β (Cizmecioglu et al., 2016; Jia et al., 2008; Ni et al., 2012; Zhang et al., 2017). Other genetic alterations may alter the p110 isoform dependency in PTEN null tumors (Schmit et al., 2014).

The contribution of p110α and p110β isoforms in brain physiology and pathology remains unknown. Recent clinical trials for PI3K inhibitors in GBM have yielded little success (Pitz et al., 2015; Wen et al., 2019). To better understand the clinical results of PI3K inhibition in GBM, we took both genetic and pharmacological approaches to explore the differential roles played by PI3K isoforms in PTEN-null GBM models. Our results demonstrate the divergent roles of PI3K isoforms in GBM and provide a possible explanation for the failure of PI3K-directed drugs in clinic and future solutions to improve therapeutic outcomes for GBM patients.

RESULTS

Either PI3K Isoform Is Sufficient for the Formation of GBM Driven by Concurrent Ablation of *Pten* and *p53*

It has been shown that concurrent deletion of *Pten* and *Trp53 (p53)* in the brains of mice resulted in high-grade gliomas that recapitulate the pathology and biology of human GBM (Zheng et al., 2008). To examine the specific roles of p110α and p110β in a murine GBM model driven by the loss of *Pten* and *p53*, we generated compound mouse strains with floxed alleles of *Pten* and *p53* along with floxed alleles of *Pik3ca* (encoding p110α) and/or *Pik3cb* (encoding p110β) as the following: $p53^{f/f};Pten^{f/f}$ (PP), $p53^{f/f};Pten^{f/f};Pik3ca^{f/f}$ (PPA), $p53^{f/f};Pten^{f/f};Pik3cb^{f/f}$ (PPB), and $p53^{f/f};Pten^{f/f};Pik3ca^{f/f};Pik3cb^{f/f}$ (PPAB). To delete the floxed alleles in the brains of the resulting mice, a viral vector encoding Cre recombinase (AdCre) was injected intracranially to the sub-ventricular zone (SVZ) region that contains a high density of neuronal stem cells/neuronal progenitor cells (NSCs/NPCs) (Bonaguidi et al., 2011; Ming and Song, 2011). The PP-AdCre mice developed brain tumors that are histologically consistent with GBM (referred to as PP tumors; Figure 1A) with a median survival of 206 days (Figure 1B). Ablation of either p110α or p110β alone delayed the development of brain tumors (PPA or PPB tumor). Mice bearing PPA or PPB tumors had

modestly prolonged survival, with median survival of 276 and 239 days, respectively (Figure 1B). However, ablation of both p110α and p110β completely blocked glioma formation in PPAB mice (Figure 1B). These data suggest that, while either PI3K isoform can support the development of PP GBM, blockade of both isoforms is required to block the gliomagenesis driven by the concurrent loss of *Pten* and *p53* in mice.

We next characterized primary mouse tumor cell lines established from PP, PPA, and PPB tumors *ex vivo*. PPA and PPB tumor cells have absent p110α or p110β protein, respectively (Figure 1C). However, the phosphorylation levels of Akt and S6RP, two well-characterized downstream signaling molecules, were not significantly altered by ablation of either isoform alone (Figure 1C), suggesting that ablating either isoform alone is not sufficient to block PI3K signaling in PP GBM cells.

To obtain PPAB tissues for the pathway signaling analysis (since no PPAB glioma available for the analysis), we isolated embryonic NSCs/NPCs from PP, PPA, PPB, and PPAB mice and cultured them briefly to introduce a retroviral vector expressing *Cre-ER^{t2}* into these cells. The Cre-ER^{T2} fusion protein is inactive until cells are treated with the synthetic estrogen antagonist 4-hydroxytamoxifen (4-OHT). This inducible knockout approach allowed us to delete *Pten, p53, p110α*, or *p110β* upon 4-OHT treatment (Figure S1A). Notably, the phosphorylation levels of Akt and S6RP were significantly reduced only by ablating both isoforms (Figure S1A). Consistent with our observation in PPA and PPB tumor cells above, ablation of either isoform alone underwent little change in the phosphorylation levels of Akt or S6RP (Figure S1A). Our genetic studies suggest that both isoforms are active in the PP GBM model.

The p110β Isoform Contributes to the Migration of PTEN Null GBM Cells

The characterization of PP, PPA, and PPB tumors by immunohistochemistry (IHC) showed that all of these tumors expressed the glioma markers GFAP and Olig2 (Figure 1A). Cellular proliferation was high across all of the samples, as indicated by IHC staining for Ki67, a marker of proliferation (Figure 1A), resembling GBM pathology in the clinic. Notably, while all of the PP and PPA tumors were highly diffusive, some of the PPB tumors displayed defined borders with neighboring tissues (Figure 1A, H&E), suggesting that the loss of p110β rendered tumors less invasive.

Given the distinct histological phenotypes of PPA and PPB tumors, we sought to determine the isoform-specific dependence of migration/invasion. Using a transwell migration assay, we showed that PPB tumor cells, but not PPA tumor cells, have significantly reduced migration (Figure 1D), supporting the *in vivo* observation that PPB tumors appeared less invasive. It has been shown that p110β interacts with Rac1/Cdc42 through its RBD domain (Fritsch et al., 2013; Yuzugullu et al., 2015). Ectopic expression of wild-type (WT) p110β restored migration in PPB tumor cells. However, a p110β mutant that is unable to bind Rac1/Cdc42 had a statistically significant but partially restorative effect on the migration of PPB tumor cells (Figures 1E and S1B), suggesting that the interaction of p110β with Rac1 plays a role in the migration and invasion of PP tumors. Furthermore, AZD6482 (also known as KIN193, p110β-selective inhibitor) and GDC0941 (pan-PI3K inhibitor), but not BYL719 (p110α-selective inhibitor) (Table S1), significantly reduced the cell migration of PP cells in

a transwell assay (Figure 1F). Our results suggest that our PP GBM model depends mostly on p110β for cell migration.

We next examined the roles of PI3K isoforms in PTEN null GBM patient-derived cell lines (PDCLs) BT179 and BT224 (Tables S2 and S3), using isoform-selective PI3K inhibitors, on their migration behavior. Notably, both PDCLs have p53 mutations concurrent with PTEN deficiency. We also observed that AZD6482 and GDC0941, but not BYL719, significantly reduced the cell migration of BT179 and BT224 cells (Figure 1G), suggesting that p110β also contributes to the migration of patient-derived GBM cells, which is consistent with the data from our murine PP GBM model.

Either PI3K Isoform Can Support the PI3K Signaling and Proliferation of PP GBM Cells *Ex Vivo*

We next used PI3K inhibitors to explore the specific roles of p110α and p110β in a panel of primary mouse GBM cells lines derived from PP, PPA, and PPB tumors *ex vivo*. While GDC0941 reduced phosphorylation levels of both Akt and S6RP in tumor cells, neither BYL719 nor AZD6482 significantly reduced the phosphorylation levels of Akt and S6RP in PP glioma cells (Figure 2A, left panel). We further showed that AZD6482 inhibited the pAkt and p6RP in PPA tumors where p110α is ablated, and vice versa, BYL719 inhibited the pAkt and p6RP in PPB tumors where p110β is ablated (Figure 2A, center and right panels). These results suggest that either isoform can activate the PI3K-Akt-S6RP signaling in these Pten null GBM cells.

A previous study has shown that PIP3 levels do not always correlate with pAkt levels (Costa et al., 2015). We assessed PIP3 levels in PP cells upon treatment with BYL719, AZD6482, or GDC0941. GDC0941 significantly reduced the PIP3 level in PP tumor cells, as expected. BYL719 or AZD6482 also significantly reduced the PIP3 levels in PP cells, despite few changes in the pAkt and pS6PR levels in these cells (Figure S2A). While the mechanism underlying this discordance of the levels of PIP3 and pAkt observed in this study and by others remains to be investigated, this result suggests that both isoforms are active in terms of producing PIP3.

To further assess the roles of PI3K isoforms in established PP GBM, we used a CRISPR system to knock out *Pik3ca* or *Pik3cb* in PP tumor cells to generate isogenic cell lines lacking either p110α or p110β, called PP-sgGFP, PP-αKO, and PP-βKO (Figure S2B). Signaling analyses showed that these tumor cells have responses to various PI3K inhibitors similar to these PP, PPA, and PPB tumor cells, respectively (Figure S2B).

Proliferation analyses of these isogenic cell lines showed that PP-αKO cells have a slower growth rate than that of PP-sgGFP or PP-βKO cells (Figure 2B). Consistent with this result, BYL719, but not AZD6482, had a modest but statistically significant effect on the proliferation of PP-sgGFP cells (Figure 2B). Again, the pan-PI3K inhibitor GDC0941 most significantly suppressed the proliferation of all PP-sgGFP, PP-αKO, or PP-βKO cells (Figure 2B). These data indicate that either isoform is sufficient for PI3K signaling and proliferation of established PP GBM cells. Notably, p110α may play a relatively more prominent role than p110β in terms of tumor cell proliferation.

We next explored the roles of PI3K isoforms in the PTEN null GBM PDCLs BT179 and BT224 (Tables S2 and S3) by examining the effects of PI3K inhibitors on their signaling and growth. Treatment with BYL719 or AZD6482 alone had only marginal effects on p-Akt^{473} and p-S6RP levels in BT179 or BT224. In contrast, GDC0941 significantly reduced p-Akt and p-S6RP levels (Figure 2C). Proliferation analyses of both PDCLs showed that they were more resistant to isoform-specific PI3K inhibitors than to the pan-PI3K inhibitor, suggesting that patient PTEN-null GBM cells can use either p110α or p110β to maintain signaling and proliferation (Figure 2D). These data suggest that our murine PP GBM model recreates the PI3K-isoform dependencies of human GBM.

Either PI3K Isoform Can Support the Signaling and Growth of Subcutaneous PP Tumors *In Vivo*

To investigate the isoform dependency *in vivo*, we examined the effects of PI3K inhibitors on the growth of PP GBM allografts. Because none of the currently available isoform-selective inhibitors are known to penetrate the blood-brain barrier (BBB), we assessed the antitumor activity of PI3K inhibitors on subcutaneous PP GBM transplants in nude mice. Tumor-bearing mice were treated with either BYL719 or AZD6482 alone, or in combination. Both BYL719 and, to a lesser degree, AZD6482 inhibited tumor growth and reduced tumor weight, but combined treatment with BYL719 and AZD6482 was able to flatten the PP tumor growth curve (Figures 3A and 3B). Western blot (WB) and IHC analyses of tumor tissues revealed that, whereas BYL719 and AZD6482 had a modest or little effect on reducing pAkt and pS6RP levels, the combined treatment of BYL719 and AZD6482 effectively blocked phosphorylation of both Akt and S6RP (Figures 3C and S3). These data are consistent with our genetic and pharmacological inhibition findings above and suggest that the inhibition of PP growth requires simultaneous blockade of both isoforms.

Limited Efficacy of BKM120 on Orthotopic PP GBM Model

We next used intracranial orthotopic allografts of PP GBM to examine BKM120 (also known as buparlisib; Table S1). BKM120 is currently the only pan-PI3K inhibitor with proven brain penetration and has been tested in the clinic for GBM patients (Wen et al., 2014). Treatment with BKM120 prolonged the median survival of PP-bearing mice slightly from 22 to 27 days (Figure 4A). While this result is statistically significant, it is unlikely to have a meaningful clinical impact. WB and IHC analyses of tumors harvested from experimental mice showed that BKM120 modestly reduced phosphorylation of both Akt and S6RP (Figures 4B and 4C), suggesting that while BKM120 can cross the BBB, it cannot deeply suppress Akt-mammalian target of rapamycin (mTOR) signaling. Our data are consistent with a recent clinical trial that showed that BKM120 does not effectively suppress S6RP phosphorylation despite adequate brain penetration and has limited efficacy in patients with GBM (Wen et al., 2019).

We hypothesized that the modest effect observed here and in clinical trials for BKM120 in GBM may be due to its relatively weak inhibition of p110β (Table S1). To test this hypothesis genetically, we compared the efficacy of BKM120 on mice bearing PP, PPA, or PPB tumors. As shown in Figure 4A, BKM120 failed to prolong the median survival of

PPA-bearing mice (26 versus 24 days). In contrast, BKM120 significantly prolonged the median survival of PPB-bearing mice to a much greater extent (Figure 4A, 37 versus 61 days). Consistent with our earlier observations that p110β contributes to GBM diffusive phenotype (Figures 1A and 1D), BKM120 treatment did not decrease the diffusive feature of PPA tumors (Figure S4). We further show that BKM120 failed to affect the migration of PP cells in a transwell assay (Figure 4D). Our data thus indicate that BKM120, although developed as a pan-PI3K inhibitor, has limited activity in our PP GBM due to the inadequate inhibition of p110β activity.

DISCUSSION

The mechanisms by which genetic context and tumor type determine PI3K isoform dependency in PTEN-deficient cancer remain elusive. Therefore, genetic identification of PI3K isoform dependency for a given tumor type can be illuminating. Our studies using genetically defined mouse models of GBM have revealed that either isoform is sufficient to support the PI3K signaling and tumor growth in the Pten null setting with concurrent loss of p53 in the tumor. Similar results were observed in patient-derived PTEN-deficient GBM cells with coexisting p53 mutations.

Our data in GBM are in contrast to the selective activation of p110β that we and others have previously observed in a variety of PTEN-null tumors. Most tumors do not use both p110α and p110β for survival. Typically, p110α activity is required in tumors driven by hyperactive RTK signaling or by oncogenes such as KRas, while p110β activity is required in tumors in which PTEN-loss is the driving event (Thorpe et al., 2015). Sometimes PI3K isoforms play spatially differential roles in tumorigenesis, such as in the skin epidermis under conditions of PTEN-loss; in this case, p110α is critical in suprabasal cells, whereas p110β is important in basal cells (Wang et al., 2013). The requirement for p110α in RTK and oncogene-driven tumors appears to arise from its higher catalytic specific activity compared to p110β. How p110β is selectively activated in many types of *Pten*-null tumors cells remains unclear. Several hypotheses have been discussed recently elsewhere (Zhang et al., 2017). In the present study, our data clearly suggest that in brain tumors, both RTK and GPCR signaling may be involved in eliciting the activation of both isoforms when PTEN removes the “brake” from the PI3K activity. Exactly which RTK(s) and GPCR(s) are activated in our GBM model remains to be determined.

Since much of our data stems from KO of either of the p110 isoforms, it is important to consider whether KO itself could be affecting the results. It is known that altering the ratios of p110α and p110β can have unexpected effects on biology (Thorpe et al., 2017; Utermark et al., 2012). It is also widely known that p110β has significant functions that are independent of its kinase activity, whereas KO either p110α or p110β (Bi et al., 2002; Bi et al., 1999) or knockin kinase-dead p110α (Foukas et al., 2006) results in early embryonic lethality in mice. However, kinase-dead p110β knockin mice can survive to adulthood, although with some defects in biological functions (Ciraolo et al., 2008). Such differences suggest that protein-protein interactions involving p110β can contribute to cellular signaling and biological functions. Furthermore, the important conclusions in this work have been

duplicated using both genetic and pharmacological ablation of p110α/β, making it likely that our observations are also the result of the catalytic function of each enzyme.

To date, PI3K inhibitors such as BKM120 have displayed limited efficacy against GBM in clinical trials (Wen et al., 2019). One major challenge for targeted therapy, especially using a combination of two or more drugs, is the on-target toxicity of the drug, since the targets of targeted therapies tend to be also important in normal physiology. Due to this type of toxicity, many inhibitors cannot be used at high enough doses to successfully inhibit tumor growth. GBMs present a special hurdle due to the BBB. At present, few PI3K inhibitors have significant brain penetration to reach a sufficient concentration in the brain. The lack of data regarding the tumor-type specific dependencies on signaling pathways also poses a challenge for targeted therapies. Our data indicate that PTEN-deficient GBMs can depend on either isoform for survival. However, most of the available “pan”-PI3K inhibitors are known to inhibit p110α potently but display relatively weak inhibition of p110β. Our preclinical study using PPB tumors strongly suggests that the limited efficacy for BKM120 in GBM is due to its failure to inhibit p110β activity effectively. Thus, effective treatment of PTEN-deficient GBM using PI3K inhibitors will require the development of brain-penetrant inhibitors that target p110α and p110β effectively. Our work reveals that p110α and p110β not only have overlapping functions but also play divergent roles in GBM. Our data suggest that p110α plays a relatively larger role in GBM proliferation, while p110β plays a major role in tumor invasion. Prior studies show that p110α interacts with RAS and p110β interacts with Rac1 (Cizmecioglu et al., 2016; Fritsch et al., 2013), which is known to play a major role in tumor cell mobility and invasiveness. This separation of roles between the two isoforms makes targeting p110β even more important, since GBMs are characterized by their diffusive nature, which limits the effectiveness of surgical resection. A recent report suggested that BKM120 blocks GBM cell migration *in vitro*, however, through its off-target effects to reduce focal adhesions and microtubule treadmilling, not through direct inhibition of PI3K activity (Speranza et al., 2016). Under our *ex vivo* and *in vivo* conditions, BKM120 likely does not have off-target effects (Brachmann et al., 2012) and did not block GBM cell invasion and migration. Our data demonstrate that there exists an unmet need to develop a brain penetrant “true” pan PI3K inhibitor and/or a brain-penetrant, potent p110β inhibitor.

STAR METHODS

RESOURCE AVAILABILITY

Lead Contact—Further information and requests for resources and reagents should be directed to and will be fulfilled by the Lead Contact, Jean J. Zhao (jean_zhao@dfci.harvard.edu).

Materials Availability—All unique/stable reagents generated in this study are available from the Lead Contact with a completed Materials Transfer Agreement.

Data and Code Availability—This study did not generate any unique datasets or code.

EXPERIMENTAL MODEL AND SUBJECT DETAILS

Mice—*P53*$^{f/f}$ (NCI mouse repository), *Pten*$^{f/f}$ (from Hong Wu group), *Pik3ca*$^{f/f}$ (Zhao et al., 2006) and *Pik3cb*$^{f/f}$ (Jia et al., 2008) mice were backcrossed to FVB strain background for 10 generations. Those mice were intercrossed to generate the experimental mice PP (*p53*$^{f/f}$;*Pten*$^{f/f}$), PPA (*p53*$^{f/f}$;*Pten*$^{f/f}$;*Pik3ca*$^{f/f}$), PPB (*p53*$^{f/f}$;*Pten*$^{f/f}$;*Pik3cb*$^{f/f}$), and PPAB (*p53*$^{f/f}$;*Pten*$^{f/f}$;*Pik3ca*$^{f/f}$;*Pik3cb*$^{f/f}$). Stereotactic intracranial injection of adenovirus expressing Cre recombinase (AdCre) were conducted on both male and female mice at 6-11 weeks old. Male nude mice (Taconic, NCRNU-M) at 8-12 weeks old were used for subcutaneous tumor transplants and male ICR-SCID mice (Taconic, ICRSC-M) at 6-9 weeks old were used for intracranial transplants. All the animal experiments were done in accordance with NIH animal use guidelines and protocols approved by the Dana-Farber Cancer Institute Animal Care and Use Committee.

Cell lines—HEK293T cell line (American Type Culture Collection, ATCC) is maintained in DMEM supplemented with 10% FBS and 100 ug/ml penicillin-streptomycin. Primary mouse neural stem cells (NSCs) were isolated from the brain of E14.5 embryos as described(Rietze and Reynolds, 2006) and maintained in NeuroCult proliferation medium (mouse) (StemCell Technologies) with 20 ng/ml EGF. Primary mouse glioma lines were isolated from the mouse brain tumors, pipetted mechanically to dissociate the tumors and then expanded in NeuroCult proliferation medium (mouse) (StemCell Technologies) supplied with 20 ng/ml EGF, 10 ng/ml FGF and 0.0002% Heparin.

Primary human glioma lines were cultured in NeuroCult proliferation medium (human) (StemCell Technologies) with 20 ng/ml EGF, 10 ng/ml FGF and 0.0002% Heparin.

Primary glioma lines were established as below, lines-gender-age:

Primary mouse glioma lines: d333PP-male-5 m, o193PP-female-9 m, o195PP-female-8 m, I42PP and I44PP (derived from o195PP orthotopic allograft in SCID mice)-male-3 m, d177PPA-male-12 m, o18PPa-female-12 m, o42PPA-female-12 m, m972PPA-female-9 m, o149PPB-female-9 m, o150PPB-female-9 m, and m712PPB-female-9 m.

Primary human glioma line: BT179-female-age52, BT224-male-age79

METHOD DETAILS

Stereotactic intracranial injection of AdCre or cell lines—Intracranial adenovirus expressing Cre (AdCre) injections were done in mice at the age of 6-11 weeks. 1 μL of 5×10^{10} pfu AdCre (University of Iowa, Iowa City, IA) was injected at SVZ region in the right hemisphere (set bregma as 0, 0, 0, the AdCre was i.c. into anterior 0, lacteral 0.5 mm, ventral 2.5 mm) using 33 gauge needle. Cells suspended in PBS (50,000 or 100, 000 cells in 1-2 μl) were intracranially injected in the right striatum (set bregma as 0, 0, 0, the cells were i.c. into anterior 0, lacteral 2 mm, ventral 2.5 mm). Animals were monitored daily for development of neurological defects.

Production of retrovirus—pMD.G (1.4 μg), pMD.MLV (4 μg), and pMSCV-creERt2-puro (5.4 μg) (Addgene#22776) or pBabe-puro-p110β WT or pBabe-puro-p110β-S205D/K224A(p110β-MT) plasmids (5.4 μg) were transfected in 80% confluent HEK293T cells on 10 cm dish by Superfect (QIAGEN) according to the manufacturer's protocol or 40 μL PEI (1 mg/ml). The virus was harvested 2 and 3 days post-transfection and ultracentrifuged (16,000 rpm, 90 mins) to concentrate and remove the FBS medium. The virus was then re-suspended in PBS for the infection in NSCs or primary glioma cells. The cells were stably expression by puromycin selection (1 μg/ml).

Plasmids constructs and lentiviral vector production—Lentiviral sgRNA constructs were cloned in the pLentiCrisp vector (Addgene). The sgRNA sequences targeting mouse *p110α and p110β are:*

sgp110α #1: 5′-TCACCCGAAGATGGTCGTGG-3′;

sgp110α #2: 5′-ACATTCCACTAGGATTCGTG-3′;

sgp110β #1: 5′-CCCGATGTTTAACCTCCTCA-3′;

sgp110β #2: 5′-TATACGAGTCAATGTCCATG-3′.

Lentivirus preparation and transduction of cells were performed as previously described(Ni et al., 2017).

PIP3 Quantification—Cells were seeded and treated with compounds for 1 hour in T75 ultra-low flasks. PIP3 were then isolated and measured with PIP3 ELISA kit (Echelon Biosciences) according to the manufacturer's protocol.

Treatment *ex vivo* and *in vivo*—For *ex vivo* studies, compounds were dissolved in DMSO except 4-OHT (Sigma) were dissolved in 100% EtOH. For *in vivo* studies, BKM120 was dissolved in 10% NMP (Sigma)/90% PEG 300 (Sigma) and administered by oral gavage at 35 mg/kg. AZD6482 was formulated in 7.5% NMP/40% PEG400 (Sigma)/52.5% water and given intraperitoneal twice a day at 20 mg/kg. BYL719 was prepared in 0.5% methylcellulose (Sigma) /water and administered by oral gavage at 45 mg/kg.

Western blot analysis—For experiments with compound treatments *ex vivo*, primary glioma cells in 6-well plates were treated with the indicated compound at 0.5 μM or 1 μM for one hour, then the cells were lysed in SDS loading/lysis buffer as described previously (Ni et al., 2012). Tumor samples were lysed and western blot analysis was performed as previously described(Ni et al., 2012).

Immunohistochemical staining—IHC assay were performed as previously reported (Ni et al., 2012).

Transwell migration assay—Primary mouse or human glioma cells (1×10^5 cells unless otherwise stated) in NeuroCult basal medium (StemCell Technologies) were seeded in transwell insert (Corning #3422) with DMEM-10%FBS medium in the bottom wells as chemoattractant. PI3K inhibitor at 2 mM were used for the treatment experiment. 1 day later, cells were fixed with 10% formalin and stained with hematoxylin (Vector lab, H3401), the

non-migrated cells on the upper side were removed with a cotton swab. Migrated cells were quantified by ImageJ software with cell counter plugin.

Tumor spheroid assay—Mouse glioma cells were seeded at the density of 100 cells per well in 384 U bottom plate (Nexcelom Bioscience) to form the tumor-spheres. The spheres were then treated with compounds (1 μM) for 6 days. The bright field images for each well were scanned using Celigo S Imaging Cytometer every other day and the tumorsphere size was determined by Celigo scanning software (Nexcelom Bioscience).

Cell viability assay—Cells were seeded in 96-well plates at a density of 1,000 cells/well and treated with serial dilutions of compounds. Cell viability was assessed after 3 days of treatment by Celltiter-Glo (Promega). Curve fitting analysis and IC_{50} value determination were performed using GraphPad Prism 8.

Subcutaneous allograft tumor growth—Each flank of athymic nude mice was injected subcutaneously with 5×10^5 cells resuspended in 20% matrigel (BD). Once the tumors reached the target size (~250 mm^3 on average), the mice were randomly regrouped and treated with PI3K inhibitors. We labeled day 1 as the day when treatment starts. Tumor size was measured every other day and volumes were calculated using the formula (length x $width^2$)/2. For pharmacodynamics studies, the mice were treated with inhibitors for 4 days and euthanized at 1 hour (AZD6482), 2 hours (BYL719), or 1 hours (combination of AZD6482 and BYL719) after the last dosing, and the tumors were collected. The samples were then processed and subject to histological examination and protein expression analysis.

QUANTIFICATION AND STATISTICAL ANALYSIS

Statistical analysis was performed by unpaired Student's t test, one-way ANOVA, two-way ANOVA, or Log-rank (Mantel-Cox) test (survival) by GraphPad Prism 8 (GraphPad Software). Data are considered significant when p values are < 0.05. * indicates p value < 0.05, ** indicates p value < 0.01, *** indicates p value < 0.001, **** indicates p value < 0.0001. All data are presented as mean ± SD unless otherwise stated.

Supplementary Material

Refer to Web version on PubMed Central for supplementary material.

ACKNOWLEDGMENTS

We thank Drs. Charles Stiles and John Alberta for providing anti-Olig2 antibody and scientific advice. We thank Victor Luu and Hanbing Guo for technical assistance. We thank Dr. Hong Wu for providing the floxed *Pten* mouse line. This work was supported in part by the National Brain Tumor Society (to J.R.M.F., P.Y.W., and J.J.Z.), NIH grants K12CA090354 (to J.R.M.F.), P01 CA142536 (to K.L.L. and J.J.Z.), P50 CA165962 (to K.L.L., P.Y.W., T.M.R., and J.J.Z.), R01 CA233810 and R35 CA231945 (to T.M.R.), and R35 CA210057 (to J.J.Z.).

REFERENCES

Bergholz JS, Roberts TM, and Zhao JJ (2018). Isoform-Selective Phosphatidylinositol 3-Kinase Inhibition in Cancer. J. Clin. Oncol 36, 1339–1342. [PubMed: 29517943]

Bi L, Okabe I, Bernard DJ, Wynshaw-Boris A, and Nussbaum RL (1999). Proliferative defect and embryonic lethality in mice homozygous for a deletion in the p110alpha subunit of phosphoinositide 3-kinase. J. Biol. Chem 274, 10963–10968. [PubMed: 10196176]

Bi L, Okabe I, Bernard DJ, and Nussbaum RL (2002). Early embryonic lethality in mice deficient in the p110beta catalytic subunit of PI 3-kinase. Mamm. Genome 13, 169–172. [PubMed: 11919689]

Bonaguidi MA, Wheeler MA, Shapiro JS, Stadel RP, Sun GJ, Ming GL, and Song H (2011). In vivo clonal analysis reveals self-renewing and multipotent adult neural stem cell characteristics. Cell 145, 1142–1155. [PubMed: 21664664]

Brachmann SM, Kleylein-Sohn J, Gaulis S, Kauffmann A, Blommers MJ, Kazic-Legueux M, Laborde L, Hattenberger M, Stauffer F, Vaxelaire J, et al. (2012). Characterization of the mechanism of action of the pan class I PI3K inhibitor NVP-BKM120 across a broad range of concentrations. Mol. Cancer Ther 11, 1747–1757. [PubMed: 22653967]

Brennan CW, Verhaak RG, McKenna A, Campos B, Noushmehr H, Salama SR, Zheng S, Chakravarty D, Sanborn JZ, Berman SH, et al.; TCGA Research Network (2013). The somatic genomic landscape of glioblastoma. Cell 155, 462–477. [PubMed: 24120142]

Cancer Genome Atlas Research Network (2008). Comprehensive genomic characterization defines human glioblastoma genes and core pathways. Nature 455, 1061–1068. [PubMed: 18772890]

Ciraolo E, Iezzi M, Marone R, Marengo S, Curcio C, Costa C, Azzolino O, Gonella C, Rubinetto C, Wu H, et al. (2008). Phosphoinositide 3-kinase p110beta activity: key role in metabolism and mammary gland cancer but not development. Sci. Signal 1, ra3. [PubMed: 18780892]

Cizmecioglu O, Ni J, Xie S, Zhao JJ, and Roberts TM (2016). Rac1-mediated membrane raft localization of PI3K/p110β is required for its activation by GPCRs or PTEN loss. eLife 5, e17635. [PubMed: 27700986]

Costa C, Ebi H, Martini M, Beausoleil SA, Faber AC, Jakubik CT, Huang A, Wang Y, Nishtala M, Hall B, et al. (2015). Measurement of PIP3 levels reveals an unexpected role for p110β in early adaptive responses to p110α-specific inhibitors in luminal breast cancer. Cancer Cell 27, 97–108. [PubMed: 25544637]

Foukas LC, Claret M, Pearce W, Okkenhaug K, Meek S, Peskett E, Sancho S, Smith AJ, Withers DJ, and Vanhaesebroeck B (2006). Critical roleforthe p110alpha phosphoinositide-3-OH kinase in growth and metabolic regulation. Nature 441, 366–370. [PubMed: 16625210]

Fritsch R, de Krijger I, Fritsch K, George R, Reason B, Kumar MS, Diefenbacher M, Stamp G, and Downward J (2013). RAS and RHO families of GTPases directly regulate distinct phosphoinositide 3-kinase isoforms. Cell 153, 1050–1063. [PubMed: 23706742]

Fruman DA, Chiu H, Hopkins BD, Bagrodia S, Cantley LC, and Abraham RT (2017). The PI3K Pathway in Human Disease. Cell 170, 605–635. [PubMed: 28802037]

Jia S, Liu Z, Zhang S, Liu P, Zhang L, Lee SH, Zhang J, Signoretti S, Loda M, Roberts TM, and Zhao JJ (2008). Essential roles of PI(3)K-p110beta in cell growth, metabolism and tumorigenesis. Nature 454, 776–779. [PubMed: 18594509]

Ming GL, and Song H (2011). Adult neurogenesis in the mammalian brain: significant answers and significant questions. Neuron 70, 687–702. [PubMed: 21609825]

Ni J, Liu Q, Xie S, Carlson C, Von T, Vogel K, Riddle S, Benes C, Eck M, Roberts T, et al. (2012). Functional characterization of an isoform-selective inhibitor of PI3K-p110β as a potential anticancer agent. Cancer Discov. 2, 425–433. [PubMed: 22588880]

Ni J, Xie S, Ramkissoon SH, Luu V, Sun Y, Bandopadhayay P, Beroukhim R, Roberts TM, Stiles CD, Segal RA, et al. (2017). Tyrosine receptor kinase B is a drug target in astrocytomas. Neuro-oncol. 19, 22–30. [PubMed: 27402815]

Pitz MW, Eisenhauer EA, MacNeil MV, Thiessen B, Easaw JC, Macdonald DR, Eisenstat DD, Kakumanu AS, Salim M, Chalchal H, et al. (2015). Phase II study of PX-866 in recurrent glioblastoma. Neuro-oncol. 17, 1270–1274. [PubMed: 25605819]

Rietze RL, and Reynolds BA (2006). Neural stem cell isolation and characterization. Methods Enzymol. 419, 3–23. [PubMed: 17141049]

Schmit F, Utermark T, Zhang S, Wang Q, Von T, Roberts TM, and Zhao JJ (2014). PI3K isoform dependence of PTEN-deficient tumors can be altered by the genetic context. Proc. Natl. Acad. Sci. USA 111, 6395–6400. [PubMed: 24737887]

Schneider CA, Rasband WS, and Eliceiri KW (2012). NIH Image to ImageJ: 25 years of image analysis. Nature Methods 9, 671–675. [PubMed: 22930834]

Speranza MC, Nowicki MO, Behera P, Cho CF, Chiocca EA, and Lawler SE (2016). BKM-120 (Buparlisib): A Phosphatidyl-Inositol-3 Kinase Inhibitor with Anti-Invasive Properties in Glioblastoma. Sci. Rep 6, 20189. [PubMed: 26846842]

Thorpe LM, Yuzugullu H, and Zhao JJ (2015). PI3K in cancer: divergent roles of isoforms, modes of activation and therapeutic targeting. Nat. Rev. Cancer 15, 7–24. [PubMed: 25533673]

Thorpe LM, Spangle JM, Ohlson CE, Cheng H, Roberts TM, Cantley LC, and Zhao JJ (2017). PI3K-p110α mediates the oncogenic activity induced by loss of the novel tumor suppressor PI3K-p85a. Proc. Natl. Acad. Sci. USA 114, 7095–7100. [PubMed: 28630349]

Utermark T, Rao T, Cheng H, Wang Q, Lee SH, Wang ZC, Iglehart JD, Roberts TM, Muller WJ, and Zhao JJ (2012). The p110α and p110β isoforms of PI3K play divergent roles in mammary gland development and tumorigenesis. Genes Dev. 26, 1573–1586. [PubMed: 22802530]

Utermark T, Schmit F, Lee SH, Gao X, Schaffhausen BS, and Roberts TM (2014). The phosphatidylinositol 3-kinase (PI3K) isoform dependence of tumor formation is determined by the genetic mode of PI3K pathway activation rather than by tissue type. J. Virol 88, 10673–10679. [PubMed: 24991009]

Wang Q, Von T, Bronson R, Ruan M, Mu W, Huang A, Maira SM, and Zhao JJ (2013). Spatially distinct roles of class Ia PI3K isoforms in the development and maintenance of PTEN hamartoma tumor syndrome. Genes Dev. 27, 1568–1580. [PubMed: 23873941]

Wen PY, Yung WKA, Mellinghoff IK, Ramkissoon S, Alexander BM, Rinne ML, Colman H, Omuro AMP, DeAngelis LM, Gilbert MR, et al. (2014). Phase II trial of the phosphatidyinositol-3 kinase (PI3K) inhibitor buparlisib (BKM120) in recurrent glioblastoma. J. Clin. Oncol. 32, 2019.

Wen PY, Touat M, Alexander BM, Mellinghoff IK, Ramkissoon S, McCluskey CS, Pelton K, Haidar S, Basu SS, Gaffey SC, et al. (2019). Buparlisib in Patients With Recurrent Glioblastoma Harboring Phosphatidylinositol 3-Kinase Pathway Activation: An Open-Label, Multicenter, Multi-Arm, Phase II Trial. J. Clin. Oncol 37, 741–750. [PubMed: 30715997]

Wen PY, Weller M, Lee EQ, Alexander BM, Barnholtz-Sloan JS, Barthel FP, Batchelor TT, Bindra RS, Chang SM, Chiocca EA, et al. (2020). Glioblastoma in adults: a Society for Neuro-Oncology (SNO) and European Society of Neuro-Oncology (EANO) consensus review on current management and future directions. Neuro-oncol. 22, 1073–1113. [PubMed: 32328653]

Yuzugullu H, Baitsch L, Von T, Steiner A, Tong H, Ni J, Clayton LK, Bronson R, Roberts TM, Gritsman K, and Zhao JJ (2015). A PI3K p110β-Rac signalling loop mediates Pten-loss-induced perturbation of haematopoiesis and leukaemogenesis. Nat. Commun 6, 8501. [PubMed: 26442967]

Zhang J, Gao X, Schmit F, Adelmant G, Eck MJ, Marto JA, Zhao JJ, and Roberts TM (2017). CRKL Mediates p110β-Dependent PI3KSignaling in PTEN-Deficient Cancer Cells. Cell Rep. 20, 549–557. [PubMed: 28723560]

Zhao JJ, Cheng H, Jia S, Wang L, Gjoerup OV, Mikami A, and Roberts TM (2006). The p110alpha isoform of PI3K is essential for proper growth factor signaling and oncogenic transformation. Proc. Natl. Acad. Sci. USA 103, 16296–16300. [PubMed: 17060635]

Zheng H, Ying H, Yan H, Kimmelman AC, Hiller DJ, Chen AJ, Perry SR, Tonon G, Chu GC, Ding Z, et al. (2008). p53 and Pten control neural and glioma stem/progenitor cell renewal and differentiation. Nature 455, 1129–1133. [PubMed: 18948956]

Highlights

- p110α and p110β isoforms of PI3K play divergent roles in PTEN-deficient GBM
- PTEN null GBM cells mainly rely on p110α for proliferation and p110β for migration
- Blockade of both p110α and p110β is necessary to effectively inhibit PTEN null GBM
- The failure of BKM120 in the clinic is likely due to its weak inhibition of p110β

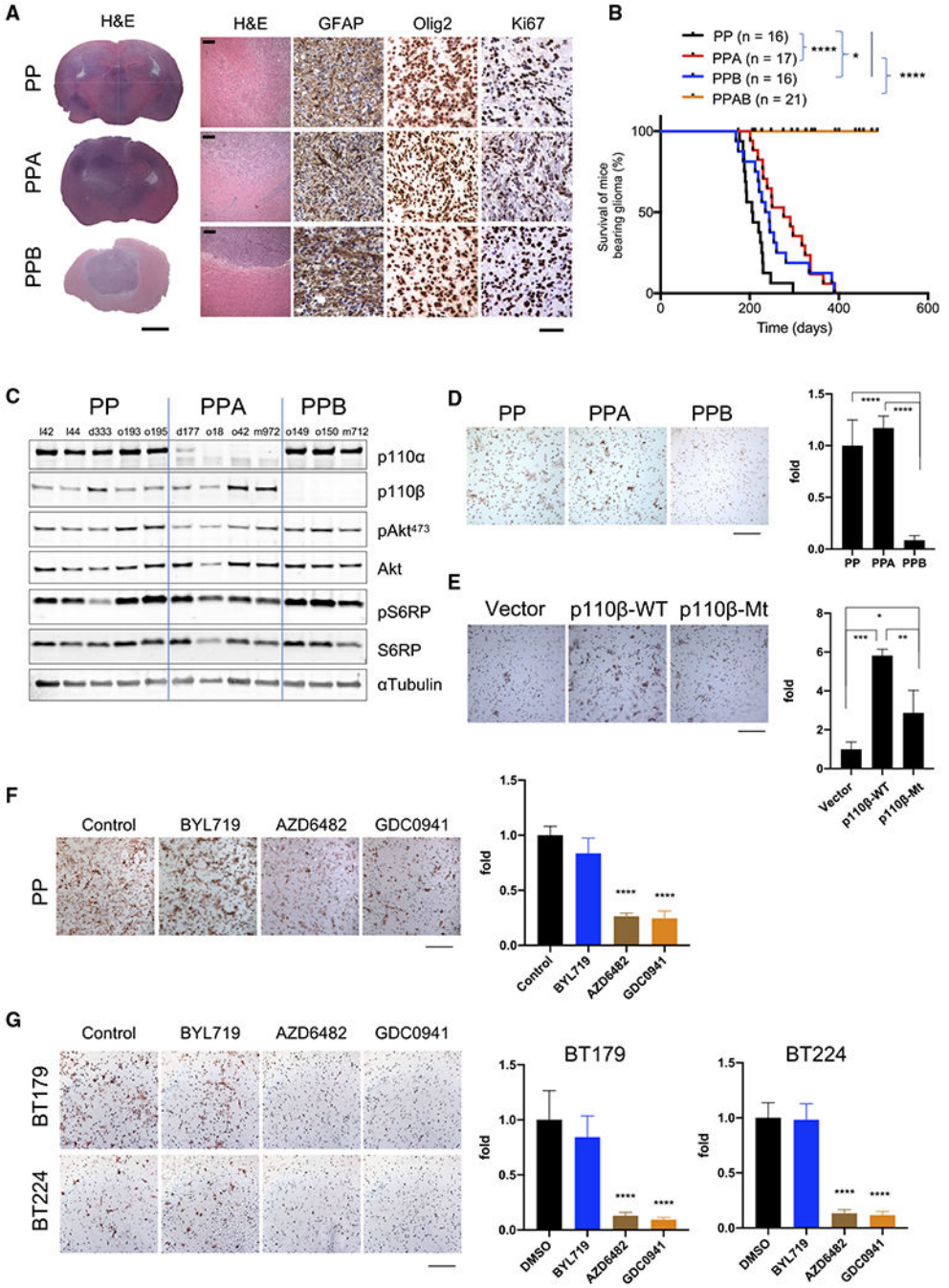

Figure 1. Either PI3K Isoform Is Sufficient for the Signaling Activation and PP GBM Formation

(A) Hematoxylin and eosin (H&E) and IHC analyses of tumors, as indicated. Representative images are shown. Scale bars, H&E (left): 2 mm; H&E (right): 400 μm; IHC: 50 μm.

(B) Kaplan-Meier (KM) survival of indicated GBM-bearing mice after intracranial injection of AdeCre (day 0). n = 16–21; *p < 0.05 and ****p < 0.0001.

(C) WB analysis of tumors, as indicated. n = 3–5/group.

(D) Transwell migration assay of primary mouse GBM cells. Representative images are shown. Scale bar, 200 mm; means ± SDs (n = 4); ****p < 0.0001.

(E) Transwell migration assay of PPB GBM cells expressing p110β-WT or p110β-MT (S205D/K224A). Representative images are shown. Scale bar, 200 μm; means ± SDs (n = 3); **p < 0.05, **p < 0.01, and ***p < 0.001.

(F) Transwell migration assay of PP GBM cells treated with indicated inhibitors. Representative images are shown. Scale bar, 200 μm; means ± SDs (n = 4); ****p < 0.0001.

(G) Transwell migration assay of BT179 and BT224 treated with indicated inhibitors. Representative images are shown. Scale bar, 200 μm; means ± SDs (n = 4); ****p < 0.0001.

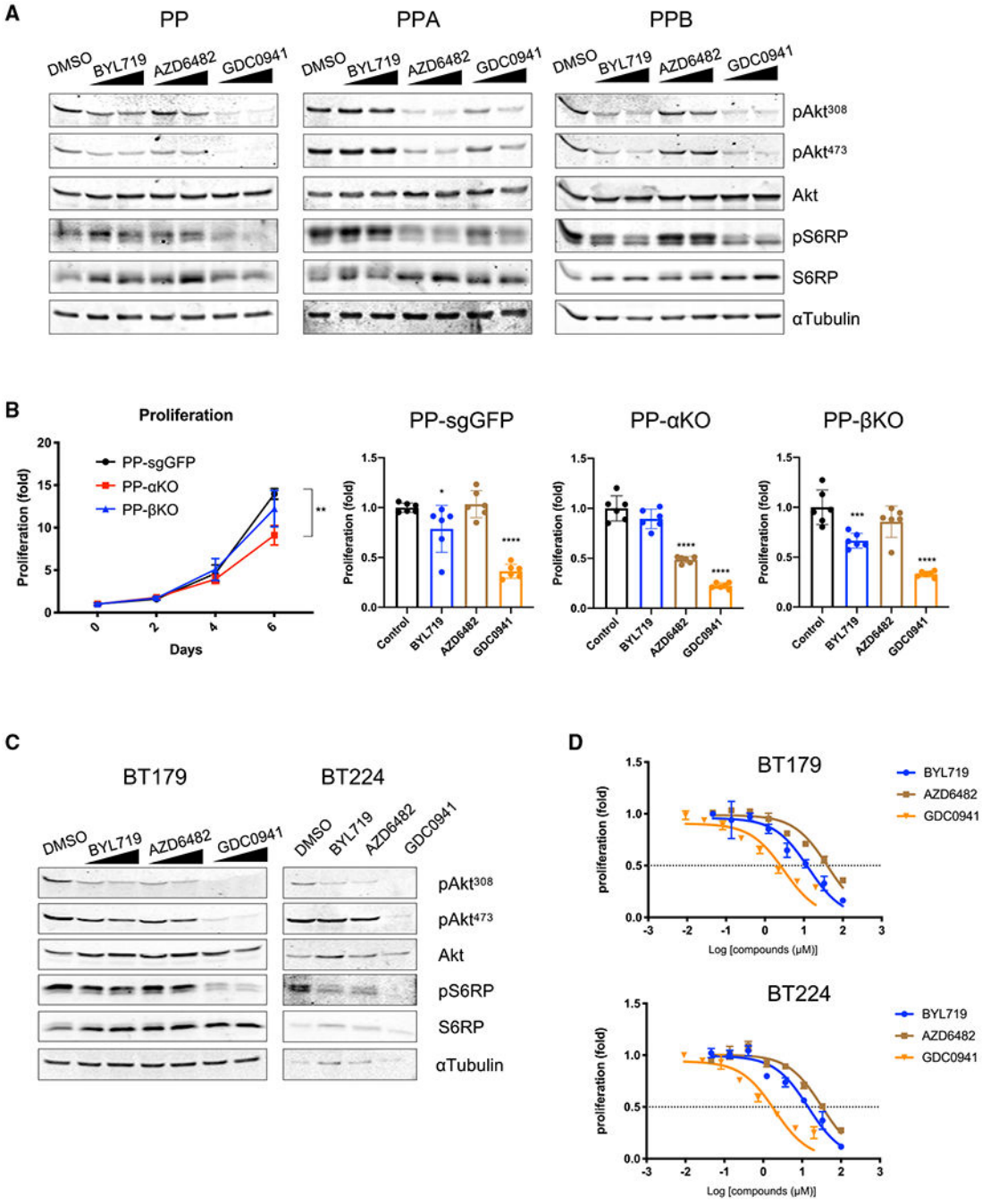

Figure 2. Either PI3K Isoform Can Support the Signaling and Proliferation of PTEN Null GBM Cells *Ex Vivo*

(A) PP, PPA, or PPB tumor cells were treated with BYL719, AZD6482, or GDC0941 and subsequently subjected to WB analysis. The data represent at least 2 different GBM lines for each tumor type.

(B) PP GBM cells were transduced with *sgPik3ca, sgPik3cb*, or control sgGFP virus. Single cells were screened to generate *PP-Pik3ca* KO (PP-αKO) or PP-*Pik3cb* KO (PP-βKO) cells. The proliferation (tumor sphere size/area) was scored as the fold to that of day 0 for each line (means ± SDs, n = 6), **p < 0.01. Right panels: cell lines were treated with the

indicated compounds and their proliferations (tumor sphere size/area) were scored as the fold to that of control for each line (means ± SDs, n = 6). *p < 0.05, ***p < 0.001, and ****p < 0.0001.

(C) BT179 and BT224 cells were treated with inhibitors, as indicated, and subsequently subjected to WB analysis.

(D) Cell viability at different does of inhibitors as determined by CellTiter-Glo assay. Means ± SDs (n = 3).

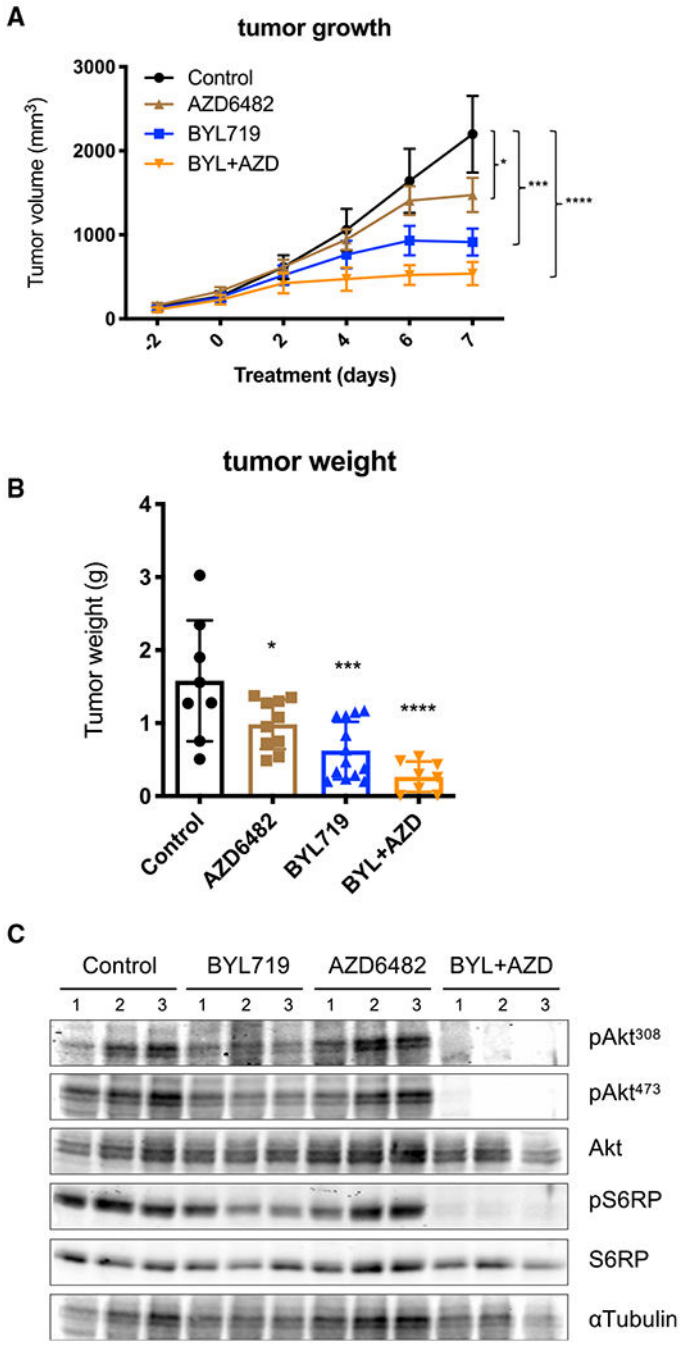

Figure 3. Either PI3K Isoform Can Support the Signaling and Growth of Subcutaneous PP Tumor *In Vivo*

(A and B) Tumor growth (A) and tumor weights (B) of PP allografts treated with inhibitors, as indicated. The data are represented as means ± SEMs(n = 8–12). *p < 0.05, ***p < 0.001, and ****p < 0.0001.

(C) WB analysis of pAkt and pS6RP on PP allografts treated with inhibitors as indicated for 4 days. n = 3/group.

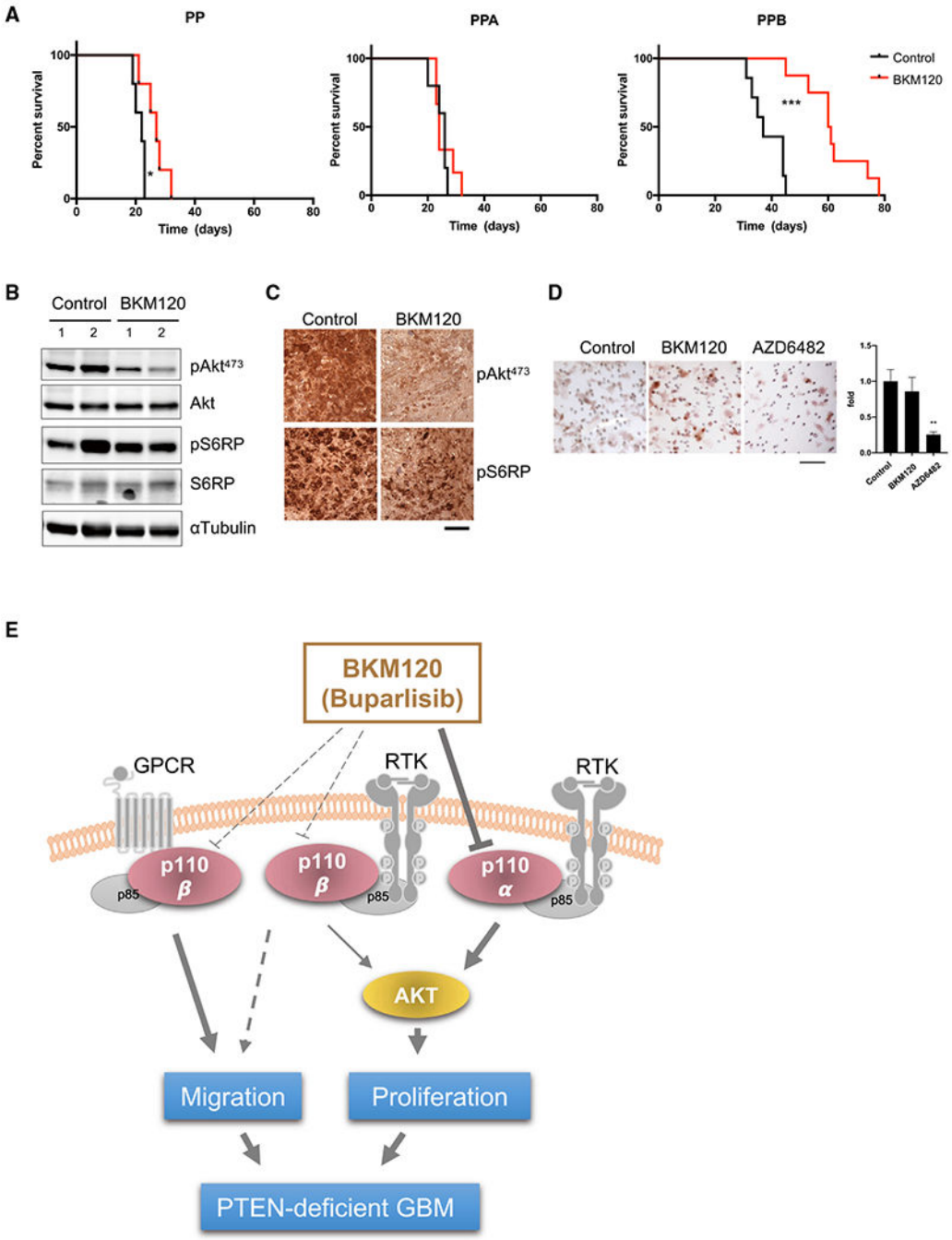

Figure 4. Limited Effect of BKM120 on Orthotopic Allografts of PP GBM

(A) KM curves of mice bearing orthotopic PP, PPA, or PPB allografts treated with BKM120 or vehicle control (n = 5–8). *p < 0.05 and ***p < 0.001.

(B) WB analysis of PP tumors from (A) at the endpoint. Tumors were collected 2 h after last dosing.

(C) IHC analysis of pAkt473 and pS6RP of orthotopic PP tumors harvested from PP-bearing mice treated with control or BKM120 for 4 days. Tumors were collected 2 h after last dosing. Scale bar, 100 μm.

(D) Transwell migration assay of PP GBM cells treated with compounds, as indicated. Representative images are shown. Scale bar, 100 μm; means ± SDs (n = 3); **p < 0.01.
(E) Divergent roles of PI3K isoforms in PTEN-deficient GBM.

KEY RESOURCES TABLE

Reagent or resource	Source	Identifier
Antibodies		
anti-p110α	Cell Signaling	Cat# 4249; RRID:AB_2165248
anti-p110β	Cell Signaling	Cat# 3011; RRID:AB_2165246
anti-pAkt(S473)	Cell Signaling	Cat# 4060; RRID:AB_2315049
anti-pAkt(T308)	Cell Signaling	Cat# 9275; RRID:AB_329828
anti-Akt	Cell Signaling	Cat# 9272; RRID:AB_329827
anti-pS6RP(S235/236)	Cell Signaling	Cat# 2211; RRID:AB_331679
anti-S6RP	Cell Signaling	Cat# 2217; RRID:AB_331355
anti-αTubulin	Sigma	Cat# T9026; RRID:AB_477593
anti-Vinculin	Sigma	Cat# V9131; RRID:AB_477629
anti-Ki67	Cell Signaling	Cat# 12202; RRID:AB_2620142
anti-GFAP	DAKO	Cat# z0334; RRID:AB_10013382
anti-Olig2	Charles Stiles lab (DFCI) (Ni et al., 2017)	N/A
IRDye 800CW goat anti-mouse IgG	LICOR Biosciences	Cat# 926-32210; RRID:AB_621842
IRDye 680CW goat anti-rabbit IgG	LICOR Biosciences	Cat# 926-68021; RRID:AB_10706309
Bacterial and Virus Strains		
Ad5CMVCre	University of Iowa	VVC-U of Iowa-5
Chemicals, peptides, and recombinant proteins		
BKM120 (Buparlisib)	MedChemexpress	CAS 1312445-63-8
BYL719	MedChemexpress	CAS 1217486-61-7
AZD6482	MedChemexpress	CAS 1173900-33-8
GDC0941	MedChemexpress	CAS 957054-33-0
CAL101	MedChemexpress	CAS 870281-82-6
4-OHT	Sigma	Cat# H7904
NMP	Sigma	Cat# 443778
PEG300	Sigma	Cat# 81162
PEG400	Sigma	Cat# 81172
Methylcellulose	Sigma	Cat# m0555
DMSO	Sigma	Cat# D8418
Superfect	QIAGEN	Cat# 301305
PEI	Polysciences	Cat# 23966
EGF	Sigma	Cat# E9644
FGF2	Miltenyi Biotec	Cat# 130-093-564
Herapin	StemCell Technologies Inc.	Cat# 07980
Critical Commercial Assays		
Celltiter-Glo	Promega	G9242
PIP3 Mass Elisa kit	Echelon Biosciences	K-2500S

Reagent or resource	Source	Identifier
Experimental Models: Cell Lines		
BT179	Dr.Keith Ligon lab (DFCI)	N/A
BT224	Dr.Keith Ligon lab (DFCI)	N/A
Primary mouse PP glioma cells	This paper	N/A
Primary mouse PPA glioma cells	This paper	N/A
Primary mouse PPB glioma cells	This paper	N/A
Experimental Models: Organisms/Strains		
p53$^{f/f}$;*Pten*$^{f/f}$ (PP) mice	This paper	FVB
p53$^{f/f}$;*Pten*$^{f/f}$;*Pik3ca*$^{f/f}$ (PPA) mice	This paper	FVB
p53$^{f/f}$;*Pten*$^{f/f}$;*Pik3cb*$^{f/f}$ (PPB) mice	This paper	FVB
p53$^{f/f}$;*Pten*$^{f/f}$; *Pik3ca*$^{f/f}$;*Pik3cb*$^{f/f}$ (PPAB) mice	This paper	FVB
Nude mice	Taconic	NCRNU-M
SCID mice	Taconic	ICRSC-M
Recombinant DNA		
pLentiCrisp-sgp110α#1	This paper	N/A
pLentiCrisp-sgp110α#2	This paper	N/A
pLentiCrisp-sgp110β#1	This paper	N/A
pLentiCrisp-sgp110β#2	This paper	N/A
pBabe-puro-p110β	Yuzugullu et al., 2015	N/A
pBabe-puro-p110β-S205D/K224A(p110β-MT)	Yuzugullu et al., 2015	N/A
pMSCV-creERt2-puro	Addgene	Cat #22776
Software and Algorithms		
PRISM8 software	Graphpad	https://www.graphpad.com
ImageJ	Schneider et al., 2012	https://imagej.nih.gov/ij/